Optimal operation of renewable energy microgrids considering lifetime characteristics of battery energy storage system

Muhammad Faisal Shehzad and Florimond Gueniat

***Abstract*— The battery energy storage system's integration with renewable energy (RE) micro-grids play an important role in solving power supply problems. To achieve reliable and economic operations of a RE micro-grid, in addition to maximize the integration of of renewable resources, the lifetime characteristics of a battery energy storage system also need to be fully investigated.**

This research study develops an optimization model that includes battery life loss cost, states switching costs, and operation and maintenance cost to obtain a set of optimal parameters of operation strategy. Considering the lifetime characteristics of battery storage system, a multi-objective optimization to maximize the power sold values, and to minimize the degradations concerning battery life cycles has been achieved being main control objectives of the research under study. Based on a model adopting mixed-integer constraints and dynamics, the problem of optimal load demand tracking, and electricity market participation is solved through the implementation of an model based predictive control (MPC) scheme. The efficacy of the proposed controller is proved through extensive simulations where the RE-based micro-grid running costs are minimized.

***Index Terms*— energy management, energy storage, MPC, optimization, battery management.**

I. INTRODUCTION

Clean energy resources in comparison to fossil fuels have raised considerable attention in energy markets during the last decade. Among them, a promising option is wind and solar [1]. However, their development is slowed down by the inherent nature of being intermittent [2].

However, the adoption of an energy storage system (ESS) combined with renewable energy sources (RES) appears to be a paradigm shift for the energy market, as it introduces new possibilities [3]. However, proper management strategies are required, the complexity of the plants increasing [4], [5].

In general, optimal operations of microgrids with RESs and battery-based ESSs are essential for their participation to the energy market especially if the operational constraints, the limitations of the ESSs, degradation, operational and maintenance costs need to be taken into account.

In practice, an energy management system (EMS) should pursue the following objectives:

- extend the battery lifetime by optimizing their working cycles;
- protect batteries from intensive use by limiting their power rates;
- track local and the contractual loads smoothly in a more feasible and economical way;
- to optimize the energy exchanged with the grid for high degree of autonomy and reducing operation and maintenance costs.

Model predictive control (MPC) is a technique that can answer these issues by providing the control inputs to safely and efficiently operate the system.

For instance, the implementation of a supervisory MPC and hybrid ESS for optimal power market management was presented in [6]. In [7], the development of model predictive control for hybrid co-generation power plants is carried out introducing the mixed logic dynamic (MLD) framework. However, the authors do not take into account other kinds of ESS nor battery degradation.

Further efforts on the optimal control strategies for the operations of wind farms/solar parks with battery-based ESSs when multiple aspects have to be addressed simultaneously, is still needed. Particularly, to the best of authors' knowledge, the reference demand tracking with the battery-based energy system to achieve stable energy production and satisfying the forecasted load demand taking into account all the operational constraints, degradation, and operational and maintenance costs, has been very little explored in the literature.

In this paper optimal operations planning of a battery-based wind farms/solar parks are investigated. The whole system exactly forms a microgrid with a local load, whose demand has to be satisfied. In order to deliver a practical control strategy, the proposed ESS economic costs and degradation are also considered. In addition, the economic benefit, from the interaction with the utility grid by selling or buying energy, is maximized. The RE microgrid is modeled by means of the MLD framework so as to comprehensively take into account for the real components' logic behavior and continuous dynamics.

Numerical simulations are performed to demonstrate the applicability and feasibility of the approach proposed against data taken from the literature. The results shows that the proposed control strategy when compared with the literature based EMSs results in battery life extension by 22%.

II. SYSTEM DESCRIPTION, MODELING AND CONSTRAINTS

Figure 1 shows the conceptual block diagram of the microgrid under investigation.

The authors are with the Department of Engineering, Birmingham City University, emails: `muhammad.shehzad3@mail.bcu.ac.uk`, `florimond.gueniat@bcu.ac.uk`

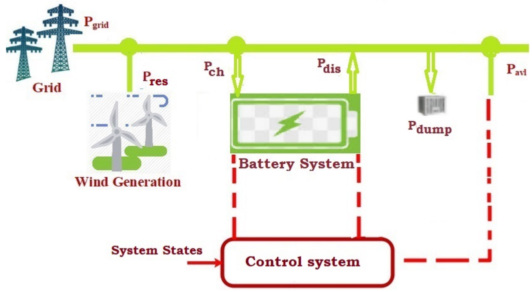

Fig. 1: Microgrid sketch. The renewable power flow, and the data flow are denoted by green and red lines, respectively. Colors available online

Under the ideal condition, the local load reference demand will be met directly from the renewables. In that case, the battery-based ESS is not operated. In real operating conditions, the excess power from the RESs is used to charge battery system, then the stored energy will be delivered to the loads in low or nearly zero wind/solar hours.

A. Model and MLD Constraints of the Battery States

The battery energy storage system modeled in the research study can be operated in 3 different physical modes, namely the on, the off and the standby modes. In order to improve readability of the proposed battery models, we introduce here some notations that will be used throughout the paper. The set $\mathcal{I} = \{\mathrm{ch}, \mathrm{dis}\}$ and the index $b \in \mathcal{I}$ will indicate the battery charging (ch) or the discharging (dis) state. The set $\mathcal{A} = \{\mathrm{NO-CH/DIS}, \mathrm{STB}, \mathrm{CH/DIS}\}$ and the index $\alpha \in \mathcal{A}$ will represents the transition between the battery modes, including the standby one.

The states $\mathrm{NO-CH/DIS}$, STB, and $\mathrm{CH/DIS}$ of the battery are derived from the mixed product between i) the associated logical variable and ii) the power relevant for that state.

For the sake of illustration, let us examine the battery in its charge state. The corresponding input power for the charge state $P_{\mathrm{ch}}^{\mathrm{in}}$ is bounded within $[P_{\mathrm{ch}}^{\min},\ P_{\mathrm{ch}}^{\max}]$. Thus, by defining $P_{\mathrm{ch}}^{\mathrm{in}} = P_{\mathrm{ch}}(k)\delta_{\mathrm{ch}}^{\mathrm{CH}}(k)$ it results $P_{\mathrm{ch}}^{\mathrm{in}} = P_{\mathrm{ch}}(k) \in [P_{\mathrm{ch}}^{\min},\ P_{\mathrm{ch}}^{\max}]$ when $\delta_{\mathrm{ch}}^{\mathrm{CH}}(k) = 1$. In addition, being mutually exclusive, all other logical variables $\delta_{\mathrm{ch}}^{\alpha}(k)$, with $\alpha \neq \mathrm{CH}$, are null. Similar conditions hold for the discharging state of the battery. The operating condition of the battery, each $\delta_b^{\alpha}(k)$ is determined as

$$\begin{cases} P_b^{\min} \leq P_b(k) \leq P_b^{\max} & \iff \quad \delta_b^{\mathrm{CH/DIS}}(k) = 1, \\ P_b(k) = P_b^{\mathrm{STB}} & \iff \quad \delta_b^{\mathrm{STB}}(k) = 1, \\ P_b(k) = 0 & \iff \quad \delta_b^{\mathrm{No-CH/DIS}}(k) = 1. \end{cases} \tag{1}$$

Since the battery will work in one and only one mode at any time k, the additional constraint

$$\delta_b^{\mathrm{NO-CH/DIS}}(k) + \delta_b^{\mathrm{STB}}(k) + \delta_b^{\mathrm{CH/DIS}}(k) = 1 \tag{2}$$

has to be considered.

The transitions among states is defined by combining the logical variables with standard logical connectives [8]. According to the number of states, there is 6 possible mode transitions.

The resulting following inequalities has been derived and provided as constraints in the proposed MPC controller:

$$\sigma_{\alpha,b}^{\beta}(k) = \delta_b^{\alpha}(k-1) \wedge \delta_b^{\beta}(k), \tag{3}$$

where $\sigma_{\alpha,b}^{\beta} \in [0, 1]$.

The modeling approach followed in this paper consists in deriving a mixed-integer formulation of the operating constraints and logical devices states ($\delta_b^{\alpha}(k)$) so as to be included in a MPC controller and numerically solved.

B. Interaction with the Utility Grid

Two states for power sale and purchase are expressed by the introduction of two logical variables $\delta^{\mathrm{pur}}(k)$ and $\delta^{\mathrm{sale}}(k)$ which are either active 1 or inactive 0. We define the set $\mathcal{S} = \{\mathrm{pur}, \mathrm{sale}\}$ and the index $g \in \mathcal{S}$ to indicate the selling and purchasing events with respect to the microgrid mode.

It follows that:

$$\delta^{\mathrm{g}}(k) = 1 \Leftrightarrow C^{\mathrm{g}}(k)P^{\mathrm{g}}(k) = P_{\mathrm{grid}}(k) \tag{4}$$

where

$$P^{\mathrm{g}}(k) = C^{\mathrm{g}}(k)P_{\mathrm{grid}}(k)\delta^{\mathrm{g}}(k), \tag{5a}$$

$$P_{\mathrm{grid}}(k) = P^{\mathrm{pur}}(k) - P^{\mathrm{sale}}(k). \tag{5b}$$

In order to avoid simultaneous power selling and buying with the grid, we introduce the following constraints:

$$\delta^{\mathrm{sale}}(k) + \delta^{\mathrm{pch}}(k) \leq 1. \tag{6}$$

C. Additional constraints

1) State Space Model of the BESS: The battery storage dynamics are defined as a function of the state of charge SOC at the previous time step SOC(k), and is modeled as dynamic equation:

$$\begin{aligned} \mathrm{SOC(k+1)} = \mathrm{SOC(k)} + \eta_{\mathrm{ch}}(\mathrm{k})\mathrm{P_{ch}(k)}\delta_{\mathrm{ch}}^{\mathrm{CH}}(\mathrm{k})\mathrm{T_s} \\ - \frac{P_{dis}(k)\delta_{dis}^{\mathrm{DIS}}(k)T_s}{\eta_{dis}(k)}, \end{aligned} \tag{7}$$

where T_s is the sampling period, the $\eta_{\mathrm{ch}}(k)$ and $\eta_{\mathrm{dis}}(k)$ are the battery charging and discharging efficiencies.

2) Feasibility and operating constraints: The power balance equations for the microgrid is:

$$P_{\mathrm{res}}(k) - P_b(k) - P_{\mathrm{grid}}(k) - P_{\mathrm{dump}}(k) = P_{\mathrm{avl}} \tag{8a}$$

$$P_{\mathrm{min,b}} \leq P_b(k) \leq P_{\mathrm{max,b}} \tag{8b}$$

$$\mathrm{SOC_{min}} \leq \mathrm{SOC(k)} \leq \mathrm{SOC_{max}}. \tag{8c}$$

P_{avl} is the remaining, available power used to meet the load requirement. P_{dump} is the hypothetical excess of power that could neither be sold nor stored.

D. The battery lifetime quantification method

The battery life time quantification method has been reported in the literature to be accurate [9], and is used in this manuscript. The constraints in Equation (9) are used to determine the BESS partial cycles. The value of partial discharge cycles (P_d) will be 1 every time the discharging process is initiated, otherwise it is 0, following [10].

$$\begin{aligned} \delta_{\mathrm{DIS}}(k) - \delta_{\mathrm{DIS}}(k-1) = 1 &\implies P_d(k) = 1, \\ \delta_{\mathrm{DIS}}(k) - \delta_{\mathrm{DIS}}(k-1) \leq 0 &\implies P_d(k) = 0. \end{aligned} \tag{9}$$

1) Depth of Discharge: The formula shown in Equation (10) is used to calculate the optimal depth of discharge (DOD) at each time interval.

$$\mathrm{DOD(k)} = 1 - \mathrm{SOC(k)}. \tag{10}$$

$$\mathrm{DOD_{max}} = \max(\mathrm{DOD(k)}). \tag{11}$$

Since a discharge vary in depth, the optimal depth of discharge at each counted partial discharge cycle at time interval k depends on the DOD at the previous time, $k-1$ and the DOD at the period k, as given in Equation (12):

$$\mathrm{DOD_{P_d}(k)} = \mathrm{DOD(k)} - \mathrm{DOD(k-1)}. \tag{12}$$

2) Estimation of BESS Lifetime: We use Miner's rule, following [9], [11], to estimate the aging of the battery. The summation of the BESS partial cycles, N_{cycles} over the planning time horizon (24h, or one day, in the present work) is compared to the maximum number of cycles CF, as provided by the manufacturer.

$$C_{\mathrm{ag}} = \frac{N_{cycles}}{\mathrm{CF}}, \tag{13}$$

where C_{ag} defines the the battery aging, while CF is the battery number of cycles to failure at maximum DOD $=$ 80% and is usually around 3000 for Li-ion batteries.

The estimation of the number of performed partial cycles is done by summing, for each discharge $\mathrm{DOD_{P_d}}$, the corresponding fraction of numbers of cycles to failure CF_{P_d} at $\mathrm{DOD_{P_d}}$. Essentially, it means associating any discharge to a fraction of a complete cycle:

$$N_{cycles} = \sum_k P_d(k)/CF_{P_d}(k). \tag{14}$$

The number of cycles to failure (CF_{P_c}) depends on DOD_{P_d}. It is obtained from the relation between life cycle and depth of discharge. Finally, the lifetime L_t of the battery, in years, is simply the inverse of the C_{ag}:

$$L_t = \frac{1}{365 \times C_{\mathrm{ag}}}. \tag{15}$$

Estimating the number of complete discharge cycles is done by comparing the L_t of a battery system to its maximum number of discharge cycles, as given by the manufacturer. The number of complete cycles per year NCC is calculated as:

$$\mathrm{NCC} = \frac{\mathrm{CF}}{L_t}. \tag{16}$$

III. System Costs

This section explains the under study microgrid overall system costs, respectively associated with the grid, the battery and the meeting the power demand.

A. Grid cost function

The cost function of the grid can be defined as follows

$$\begin{aligned} \boldsymbol{J}_{\mathrm{grid}}(k) = \Big[&- \left(\boldsymbol{C}_k^{\mathrm{sale},T-1}\right)^\top \boldsymbol{P}_k^{\mathrm{sale},T-1} \\ &+ \left(\boldsymbol{C}_k^{\mathrm{pch},T-1}\right)^\top \boldsymbol{P}_k^{\mathrm{pch},T-1} \Big] T_s, \end{aligned} \tag{17}$$

where $\boldsymbol{C}_k^{\mathrm{sale},T-1}$ and $\boldsymbol{C}_k^{\mathrm{pch},T-1}$ are column vectors containing, respectively, all the energy sale/purchase prices at each time-step k, while $\boldsymbol{P}_k^{\mathrm{sale},T-1}$ and $\boldsymbol{P}_k^{\mathrm{pch},T-1}$ are the logical power vectors required to hide the non-linearity.

B. Operating cost functions

The overall battery storage energy system is proposed as

$$\begin{aligned} J_{batt}(k) = &\left(\frac{CC_{\mathrm{bat}}}{\mathrm{Cycles_{bat}}}\right) \delta_b^{\mathrm{CH/DIS}}(k) \\ &+ \mathrm{Cost}_{\alpha,b}^{\beta} \sigma_{\alpha,b}^{\beta}(k), \end{aligned} \tag{18}$$

where CC_{bat} is the battery capital cost, $\mathrm{Cycles_{bat}}$ is the battery working cycles, $\alpha, \beta \in \mathcal{A}$, and $\alpha \neq \beta$, k is the current time instant, and the $\mathrm{Cost}_{\alpha_b}^{\beta} \sigma_{\alpha_b}^{\beta}(k)$ denote the cost associated with the battery switching modes.

C. Electric reference tracking cost function

The load tracking cost function is given by the cumulative squared error between P_{ref} and P_{avl} as

$$J_l = ||\boldsymbol{P}_{\mathrm{avl,k}}^{T-1} - \boldsymbol{P}_{\mathrm{ref,k}}^{T-1}||_2^2 \tag{19}$$

IV. Controller Design

The proposed MPC provides a trajectory of future control inputs satisfying the system dynamics and constraints and minimizing the microgrid operational costs.

Let us now introduce the set $\mathcal{C}_k$ of all the decision variable vectors at instant k defined as

$$\mathcal{C}_k := \left\{ \boldsymbol{P}_{\mathrm{b},k}^{T-1}, \boldsymbol{P}_{\mathrm{avl},k}^{T-1}, \mathbf{P}_{\mathrm{dump},k}^{T-1}, \boldsymbol{\delta}_{\mathrm{i},k}^{\alpha,T-1}, \boldsymbol{\sigma}_{\alpha,\mathrm{i},k}^{\beta,T-1}, \boldsymbol{P}_{\mathrm{grid},k}^{T-1} \right\}, \tag{20}$$

Furthermore, let us define the global cost function to be minimized by the MPC controller as

$$J(k) = \omega_{\mathrm{batt}} J_{\mathrm{batt}}(k) + \omega_{\mathrm{grid}} J_{\mathrm{grid}}(k) + \omega_{\mathrm{l}} J_{\mathrm{l}(k)}, \tag{21}$$

the positive weighting factors $\omega_{\mathrm{b}}, \omega_{\mathrm{grid}}$ and ω_{l} can be set to obtain a desired prioritization.

Therefore, the following MPC problem can be formulated

$$\begin{aligned} &\min_{\mathcal{C}_k} J(k) \\ &\text{s.t.} \\ &\quad \text{Discrete logical states (1), Mode transitions (3),} \\ &\quad \text{Grid constraints (4), Storage dynamics (7),} \\ &\quad \text{Physical constraints,Power balancing equation (8),} \\ &\quad \alpha, \beta \in \mathcal{A}, \alpha \neq \beta,\ \delta^{\mathrm{grid}} \in \{0,1\},\ \ \delta_i^{\alpha}, \sigma_{\alpha_i}^{\beta} \in [0,1], \\ &\quad b \in \mathcal{I}. \end{aligned} \tag{22}$$

V. Simulations and Numerical Results

In this section, the proposed MPC strategy is validated via numerical simulations based on the data from literature. Several (one week) power production and consumption profiles are considered so as to stress the capability of the controller to address different scenarios.

As a representative examples, both a week and a day long simulation horizon have been reported in detailed in this section.

For simulations, the parameters affecting the cost functions used by the optimizer are reported in Table 1.

TABLE 1: MPC parameters.

Li-Ion battery parameters	
$\eta_{\mathrm{ch}} = 0.90$	$\eta_{\mathrm{dis}} = 0.95$
$CC_{\mathrm{bat}} = 300\,\text{£/kWh}$	$\mathrm{Cycles}_{\mathrm{bat}} = 3000$
$\mathrm{Cost}^{\mathrm{CH/DIS}} = 0.055$ £	$\mathrm{Cost}^{\mathrm{No-CH/DIS}} = 0.055$ £
$\mathrm{Cost}^{\mathrm{STB}} = 0.0275$ £	$P_b^{\mathrm{min}} = 0.2\,\mathrm{kW}$
$P_b^{\mathrm{STB}} = 0.1\,\mathrm{kW}$	$P_b^{\mathrm{max}} = 4\,\mathrm{kW}$
Weights: $\omega_{\mathrm{batt}} = 1$, $\omega_{\mathrm{grid}} = 1$ $\omega_{\mathrm{l}} = 1$	

A. One week Result Analysis

Figure 2a shows the requested electric demand and the renewable generations considered in the case study, respectively.

The utility grid interaction developed in this research study for electricity buying and selling is shown in Figure 2d. It is possible to observe from the figure that over a 168 hours horizon, at each time-step the controller tends to sell energy to the grid and maximize the revenue by selling during the high energy selling hours, and vice versa in case of energy purchasing.

The increment in the battery SOC can be seen in Figure 2b during these hours.

B. One-day Result Analysis

In order to show the efficacy and the validation of the proposed MPC, a stressing test plant scenario among the week long simulations has been detailed.

The Figure 3a show the frequent variations of the electric demand and the renewable generations.

It is observable that during the hours of high electric demand i.e., 21-25, the controller takes decision on balancing the energy equation through renewable generations, battery SOC, and as a last resort to buy energy from the grid. The electric demand P_d has the highest priority and therefore the controller tends to meet the demand in all 24 hours of the day as can be seen from Figure 3.

Between the hours 3,4-5, 13, 15, the electric demand is less than the available system power. Therefore, in order to maximize the revenue the controller set the δ^{sale} to 1 as shown in Figure 3e.

An increment in the battery state of charge during high RES hours can be shown in Figure 3d.

It is worth mentioning here that as per the novelty of the proposed approach, at any time step k, the controller put the batteries in its standby states Figure 3d when there is a small charging or discharging battery requests available in order to avoid its frequent charging or discharging cycles.

C. Results Comparison

To further illustrate the paper results, the proposed MPC scheme is compared with the relevant literature based strategies presented in [9], [12].

Results are summarized in Table 2 concerning the life extension of the battery, and Table 3 concerning the financial impact of the present EMS. It corresponds to a 2.97 years extension of the battery life (22%), with a degradation of 11% of the sales balance, when compared to the literature approach.

It can be seen that the ON-OFF strategy results in more switching modes of the battery than the proposed strategy, as seen Figure 3f. It leads to more degradation in the battery life cycles.

As it is possible to see from Figure 3c, and the discharging cycles Figure 3f, the controller frequently sets the devices in their ON-OFF states, which leads higher life cycles degradation.

Conversely, the presented approach is able to set the devices in their stand-by states to keep the battery stacks warm and to avoid frequent charge/discharge cycles during the hours 2-7-8,12,15,18,20,22,24, as illustrated Figures 3d and 3f.

Furthermore, the average DOD for the standard approach is 37.49%, compared to 31.07% with our approach.

There is a reduction of the sales balance of 11%, however the life cycle of the EMS is prolonged by 21.7%. It corresponds, when considering the life cycle of the minigrids, of a net increase of the total revenues of 8.4%.

Influence of the battery weight: We investigated the effect of the weight ω_{batt} on the battery life and the profit earned, see Figure 4.

As expected, increasing ω_{batt} results in increasing the battery life. On the other hand, the constraints on the battery results in buying more from the grid and hence to less profit. Therefore, this may lead to an not economically viable system for the wind farm or the solar park owners. This parametric study of the influence of the weight allows owners to decide their preferred balance between economic profit, sustainability and life cycle of the system.

VI. Conclusion

In this manuscript, we proposed a novel strategy for managing a battery-based ESS integrated in a RES facility.

The proposed MPC scheme takes into account the cost that the battery introduces each time it switch between different operating modes, thus decreasing the corresponding number of life cycles and efficiencies.

In conclusion, the main results of the study are: i) the development of novel dynamic models for battery-based ESS that take into account the associated working cycle degradation; ii) the integration of the developed models into a MDL framework for an MPC strategy to control a target electricity storage plant; iii) the validation of the proposed strategy in a grid connected simulation scenario for maximization of both revenue generation and lifetime of the system; iv) the correct tracking of the local and contractual user electrical demands. In particular, the proposed methodology allows to increase the lifetime of the battery by more than 20%, with a limited impact on the sales balance and an overall improvement of the revenue over the life of the equipment.

Future works will integrate the proposed results into a multi timescale BESS power regulation market, and to deploy the control strategy to the Birmingham City University laboratory microgrid. Furthermore, a multi-parametric Pareto analysis of the impact of parameters will also be carried out in real time energy market environment.

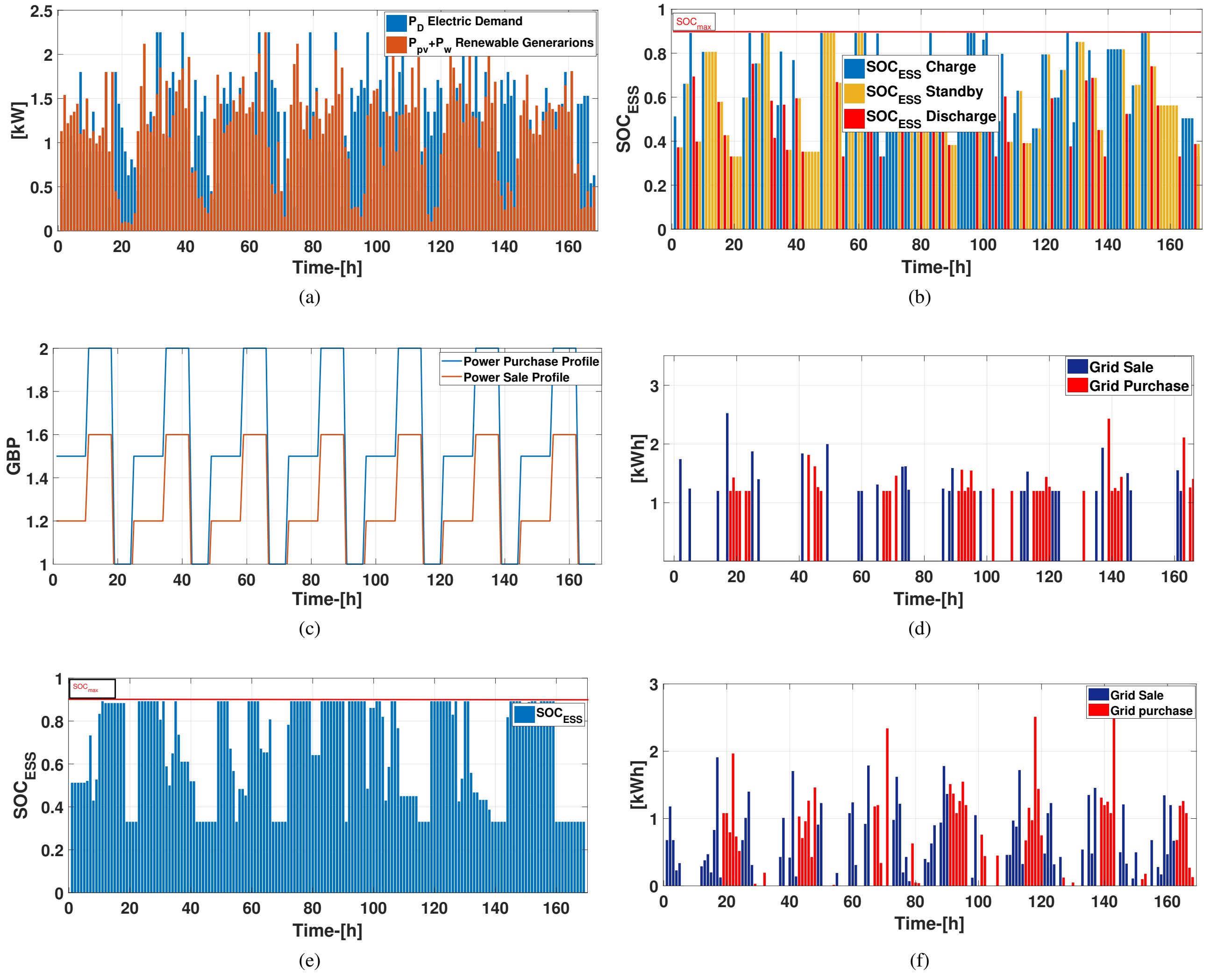

Fig. 2: Numerical results. (a) Electric demand and renewable generations. (b) Battery SOC presented. (c) Energy Price Profile. (d) Grid buying/selling. (e) Battery SOC literature. (e) Grid buying/selling literature. Colors available online

TABLE 2: Comparison of the lifetime of the battery system.

Approach	Battery working cycles	Completed cycles/year	Average DOD	L_t	Life extended (years)	Variation
Literature approach [9], [12]	3000	219.13	37.49%	13.69	-	-
Presented approach	3000	180.07	31.07%	16.66	2.97	21.7%

TABLE 3: Comparison of one-week performances. SB stands for Sales Balance.

Approach	Completed cycles/week	Average DOD	Life extended/week	Battery cycles saved/week	SB (€)	Variation
Literature approach [9], [12]	4.21	37.49%	-	-	47.5	-
Presented approach	3.46	31.07%	0.05(years)	0.75	42.3	-11.0%

REFERENCES

[1] H. Ishaq and I. Dincer, "A comparative evaluation of otec, solar and wind energy based systems for clean hydrogen production," *Journal of Cleaner Production*, vol. 246, p. 118736, 2020.

[2] A. S. Ingole and B. S. Rakhonde, "Hybrid power generation system using wind energy and solar energy," *International Journal of Scientific and Research Publications*, vol. 5, no. 3, pp. 1–4, 2015.

[3] D. Akinyele and R. Rayudu, "Review of energy storage technologies for sustainable power networks," *Sustainable Energy Technologies and Assessments*, vol. 8, pp. 74–91, 2014.

[4] C. Liu, X. Wang, X. Wu, and J. Guo, "Economic scheduling model of microgrid considering the lifetime of batteries," *IET Generation, Transmission & Distribution*, vol. 11, no. 3, pp. 759–767, 2017.

[5] J. Li, R. Xiong, H. Mu, B. Cornélusse, P. Vanderbemden, D. Ernst, and W. Yuan, "Design and real-time test of a hybrid energy storage system in the microgrid with the benefit of improving the battery lifetime," *Applied energy*, vol. 218, pp. 470–478, 2018.

[6] L. Valverde, C. Bordons, and F. Rosa, "Power management using model predictive control in a hydrogen-based microgrid," in *IECON* 38^{th} *Conference on Industrial Electronics Society*. IEEE, 2012, pp. 5669–5676.

[7] G. Ferrari-Trecate, E. Gallestey, P. Letizia, M. Spedicato, M. Morari, and M. Antoine, "Modeling and control of co-generation power plants: A hybrid system approach," *IEEE transactions on control systems technology*, vol. 12, no. 5, pp. 694–705, 2004.

[8] A. Bemporad and M. Morari, "Control of systems integrating logic, dynamics, and constraints," *Automatica*, vol. 35, no. 3, pp. 407–427,

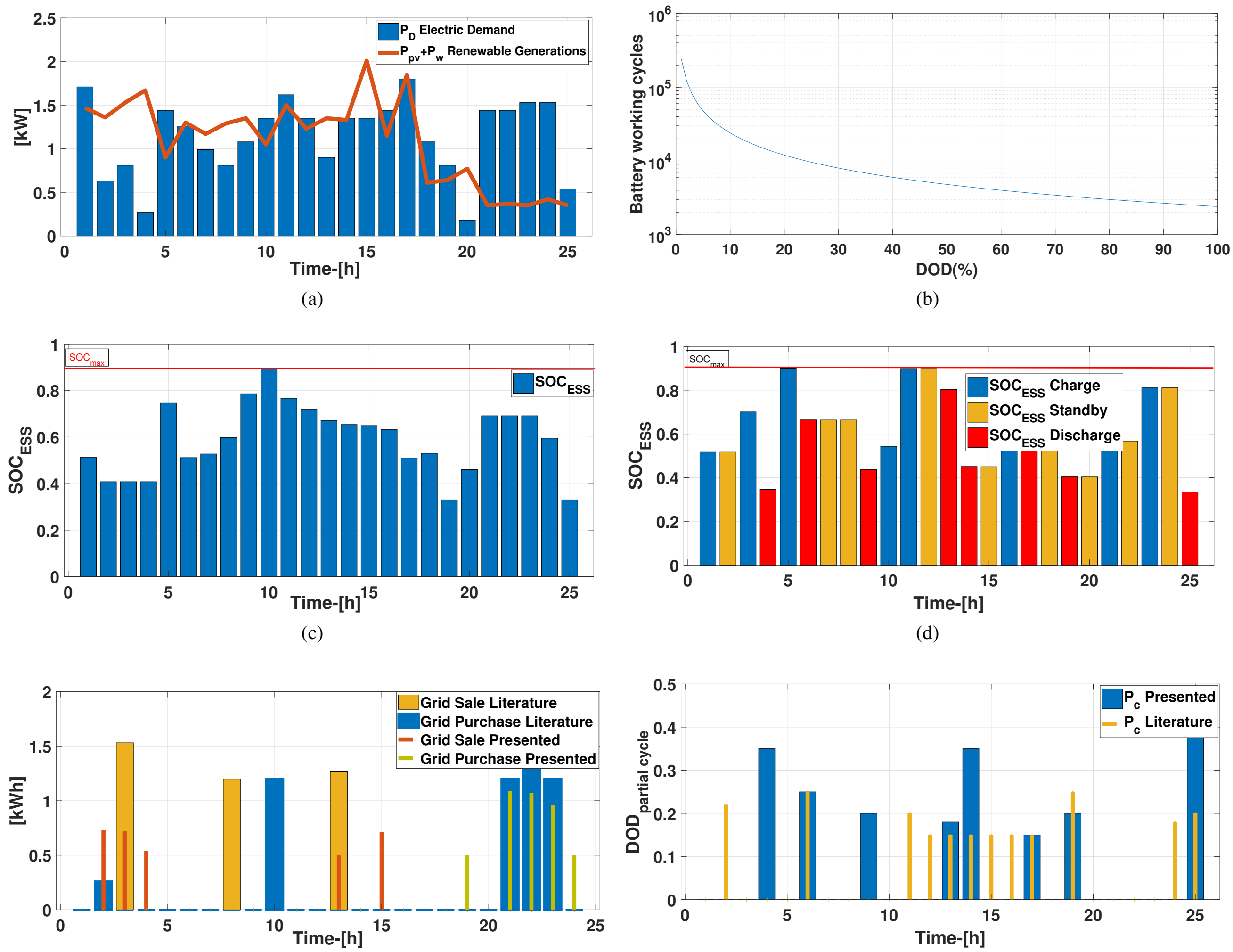

(a) (b) (c) (d) (e) (f)

Fig. 3: Numerical results. (a): Renewable generations and Load Demand. (b) Battery number of complete working cycles with respect to the DOD. (c) ESS SOC without the control strategy. (d) ESS SOC with proposed control strategy. (e): Grid Buying/selling literature and presented approach. (f): $\mathrm{DOD_{P_c}}$ with literature and presented approach.

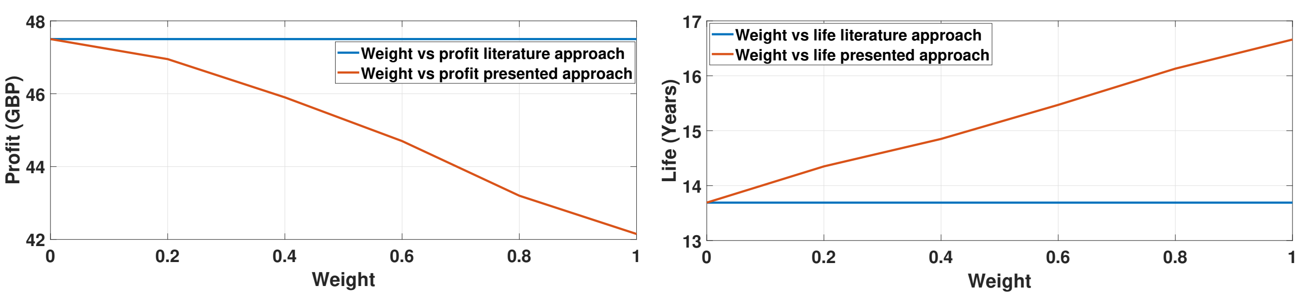

(a) (b)

Fig. 4: Numerical results. (a): Weight ω_{batt} vs. profit. (b) Weight ω_{batt} vs. battery life.

1999.

[9] T. M. Masaud and E. El-Saadany, "Correlating optimal size, cycle life estimation, and technology selection of batteries: A two-stage approach for microgrid applications," *IEEE Transactions on Sustainable Energy*, 2019.

[10] B. Xu *et al.*, "Degradation-limiting optimization of battery energy storage systems operation," 2013.

[11] S. Bahramirad, W. Reder, and A. Khodaei, "Reliability-constrained optimal sizing of energy storage system in a microgrid," *IEEE Transactions on Smart Grid*, vol. 3, no. 4, pp. 2056–2062, 2012.

[12] F. Garcia-Torres, L. Valverde, and C. Bordons, "Optimal load sharing of hydrogen-based microgrids with hybrid storage using model-predictive control," *IEEE Transactions on Industrial Electronics*, vol. 63, no. 8, pp. 4919–4928, 2016.